

Ultrashort pulses characterization by nonlinear diffraction from virtual beam

A. S. Aleksandrovsky,^{1,2,a)} A. M. Vyunishchev,^{1,2} A. I. Zaitsev,^{1,2} A. A. Ikonnikov,² and G. I. Pospelov²

¹*L. V. Kirensky Institute of Physics, 660036 Krasnoyarsk, Russia*

²*Siberian Federal University, 660079 Krasnoyarsk, Russia*

(Received 21 December 2010; accepted 20 January 2011; published online 8 February 2011)

Noncollinear frequency doubling in a random nonlinear photonic crystal of strontium tetraborate via nonlinear diffraction from virtual beam is investigated. This effect is shown to be useful for ultrashort pulses characterization in broad spectral range. Nonlinear photonic crystals of strontium tetraborate are a promising medium for ultrafast diagnostics in short-wavelength applications.

© 2011 American Institute of Physics. [doi:[10.1063/1.3554370](https://doi.org/10.1063/1.3554370)]

Progress in studies of ultrafast phenomena is directly connected with both development of ultrashort pulses generation techniques and methods of their characterization. For the latter, the nonlinear optical techniques based on noncollinear second harmonic generation are of most prevalence.^{1,2} The use of angular phase matching in this case considerably widens the dynamical range of pulses to be characterized. For diagnostics of deep and vacuum ultraviolet pulses, the achievement of angular phase matching becomes more complicated and the development of other phase matching methods becomes necessary. Different kinds of phase matching in random nonlinear media are extensively investigated in recent years. A special case of these media is nonlinear photonic crystals (NPC) that contain antiparallel ferroelectric domains with random thickness. The feature of random NPC is a broad spectrum of reciprocal superlattice vectors that contribute quasiphase matching along a wide spectrum of interacting pulses. Particularly, autocorrelation of counterpropagating waves in random NPC is investigated³ and combined action of random quasiphase matching (RQPM) and total internal reflection is studied.⁴ These papers employ strontium barium niobate as a random nonlinear medium that limits the applicability of ideas developed in them to the visible. If any of the interacting waves falls into the spectral range shorter than 270 nm, the only random nonlinear medium that can be used is strontium tetraborate (SBO). Nonlinear coefficients of SBO are highest among nonlinear crystals transparent in this range.⁵ The transparency of this crystal may be limited to 125 nm.⁶ Despite that strontium tetraborate is not proved to be a ferroelectric, antiparallel domains were found in it.⁷ Nonlinear diffraction (NLD) in random NPC of SBO was studied in Ref. 8 and wide spectral tunability of this phase matching method was demonstrated in Ref. 9. RQPM in SBO was investigated in Refs. 10 and 11 and the latter study revealed that for short-wavelength ranges, the subbands in the band structure of NPC become rather narrow, which may influence the accuracy of autocorrelation measurement. In view of this, the most promising autocorrelation geometry is the employment of nonlinear diffraction from virtual beam (NLDVB). This effect was recently discovered in artificially designed NPCs representing a superposition of several periodic superlattices¹² and in two-dimensional periodic NPC.¹³

One may expect that the same effect could be observable in as-grown NPCs with a high degree of randomization, though larger necessary peak power might be expected.

In the present communication, we report the observation of NLDVB in self-organized NPC of SBO and study the main features of background-free autocorrelation technique based on this effect. In difference with Ref. 12, the nonlinear medium in our experiment is not periodic but a random NPC. The laser source used was a femtosecond oscillator with several hundred kilowatts peak power. Another difference is the use of traditional autocorrelation optical scheme with fixed spatial and controlled temporal overlap instead of a scheme with uncontrollable temporal overlap. The sample under study was the crystal of strontium tetraborate with the dimensions $6 \times 3.5 \times 3.8$ mm³ along the crystallographic axes a , b , and c , respectively (in $Pnm2_1$ space group representation). All facets of sample are perpendicular to corresponding crystallographic axes. The sample contained one-dimensional NPC structure with domain walls perpendicular to the a axis. The radiation from Tsunami/MilleniaVs femtosecond oscillator was divided into two parallel beams that were focused with a cylindrical lens ($F=94$ mm; external angle between beams: 6.75°) into NPC. One of the beams passed optical delay line to control the arrival of the femtosecond pulse into NPC with respect to the pulse in the second beam and to ensure their temporal overlapping inside NPC. Two limiting interaction geometries are possible for nonlinear diffraction in one-dimensional (1D) NPC, as shown in Fig. 1. In the first case, the wave vectors of intersecting input radiation beams propagate in the plane orthogonal to domain walls [Fig. 1(a)] and nonlinear polarization is proportional to the largest nonlinear coefficient d_{ccc} of SBO. In the second case, the beams lie in the plane of domain walls [Fig. 1(c)] and a smaller nonlinear coefficient d_{caa} was employed. In the first case, refraction coefficients of both input and generated waves were angle-independent. In the second case, the generated wave refractive index becomes angle-dependent. The patterns of nonlinear diffraction for 800 nm central wavelength of input radiation are presented in Fig. 2 and illustrate sensitivity to the geometry of beams propagation.

Figures 2(a)–2(e) present NLD patterns for propagation in the plane perpendicular to domain walls, the geometry that was not investigated in Ref. 12. Every two fundamental

^{a)}Electronic mail: aleksandrovsky@kirensky.ru.

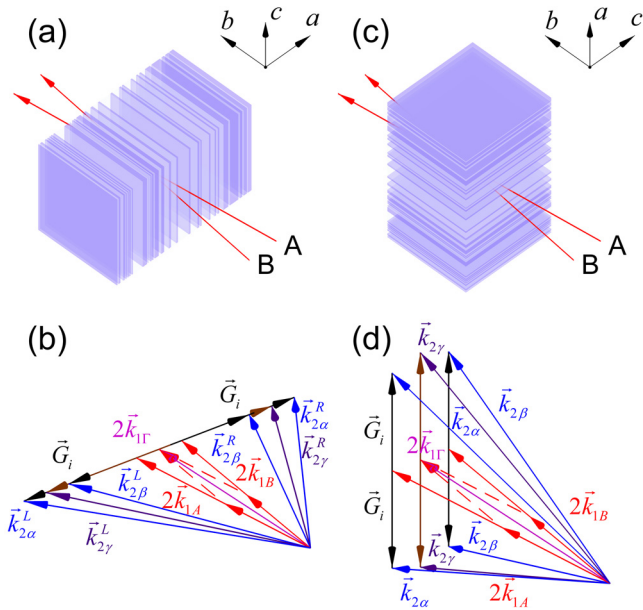


FIG. 1. (Color online) Experimental geometries and corresponding noncolinear phase matching diagrams in NPC of SBO. Input beams lie in the [(a) and (b)] ab crystallographic plane and in the [(c) and (d)] bc plane.

beams denoted by A and B produces two NLD second harmonic beams lying to the left and to the right from the corresponding fundamental beam; however, if incidence angles of A and B beams are equal, left and right nonlinearly diffracted beams from A and B fundamental beams overlap, due to mirror symmetry, and only two NLD spots are seen [Fig. 2(a)]. Overlapping is broken when we rotate NPC [for instance, clockwise by 8° in Fig. 2(b)]. Blocking whether the A or B beam proves that second harmonic (SH) spots with larger NLD angle (α) correspond to the right (A) fundamental beam [Fig. 2(c)], while spots with smaller NLD angle (β)

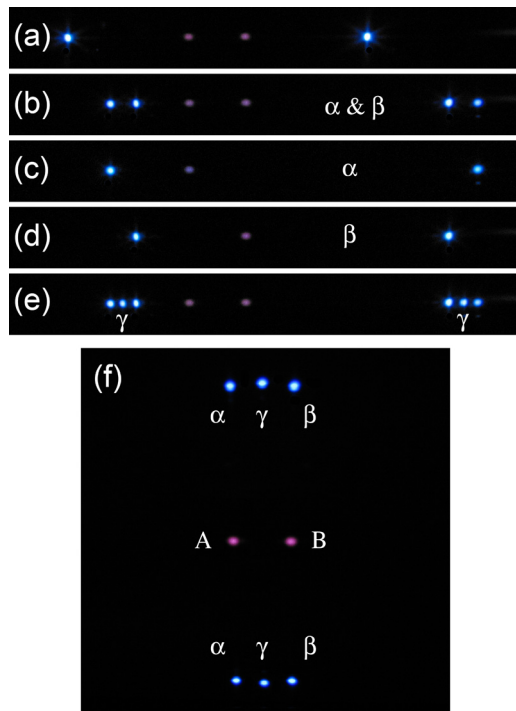


FIG. 2. (Color online) Nonlinear diffraction patterns in 1D NPC for geometry in [(a)–(e)] Fig. 1(a) and in (f) Fig. 1(c).

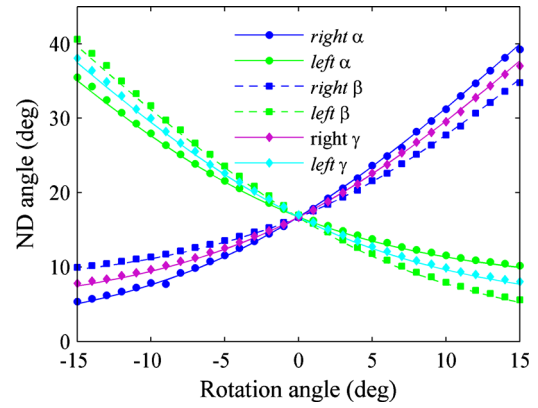


FIG. 3. (Color online) Experimental (points) and calculated (lines) dependences of NLD angles on the NPC rotation angle in geometry from Fig. 1(a). The middle sets of data correspond to NLD from virtual beam.

are nonlinearly diffracted from the left beam [Fig. 2(d)]. For anticlockwise rotation, this situation becomes symmetrically inverted. Tuning the delay allows to adjust temporal overlap of both fundamental beams and SH spot γ from the virtual beam appears [Fig. 2(e)]. Note that for this case [Fig. 1(a)], the spot diffracted from the virtual beam is seen separately only in case of angular mismatch between domain walls and wave vector of virtual beam.

External propagation angles of two SH beams nonlinearly diffracted from virtual beam can be found from phase matching diagram (Fig. 1)

$$\theta_{2\gamma} = \arcsin \left[\sqrt{n_2^2 - \frac{1}{4}(\sqrt{n_{1A}^2 - \sin^2 \theta_{1A}} + \sqrt{n_{1B}^2 - \sin^2 \theta_{1B}})^2} \right] \pm \varphi, \quad (1)$$

where $\theta_{1A,B}$ are the external incidence angles of fundamental beams A and B onto NPC input facet and $\varphi = (\theta_{1A} + \theta_{1B})/2$ is NPC rotation angle.

Calculated and experimental dependences of NLD angles are presented in Fig. 3, the SH diffracted from the virtual beam being the middle sets of data. Randomness of the NPC under study is the factor that enables observability of NLD in the wide range of rotation angles, due to wide reciprocal superlattice vector spectrum.

The NLD pattern for geometry in Fig. 1(c) identical to the case¹² is presented in Fig. 2(f) for zero NPC rotation angle. In this case, we also obtained agreement between experimental NLD angles (17.5° for NLD from individual beams and 17.8° for NLDVB) and calculated ones (17.6° and 18° , correspondingly).

For autocorrelation measurements, we employed the geometry according to Fig. 1(a) to employ the largest SBO nonlinear coefficient. The position of NPC was adjusted to find better reciprocal superlattice spectrum and to maximize the NLDVB signal. Rotation angle φ was chosen to be 8° . The SH average power was measured with Newport (Irvine, CA) 918UV/1931C detector with BG39 filter installed in front of it. Varying the delay between input fundamental beams results in autocorrelation function presented in Fig. 4 (empty circles). For the comparison, we used 0.5 mm thick beta barium borate (BBO) crystal cut in the direction of angular phase matching (solid line with dots). The pulse duration measured using NPC SBO was 82.1 fs, while that measured with BBO was 81.8 fs. The broadening of pulses under measurement in both nonlinear media can be neglected.

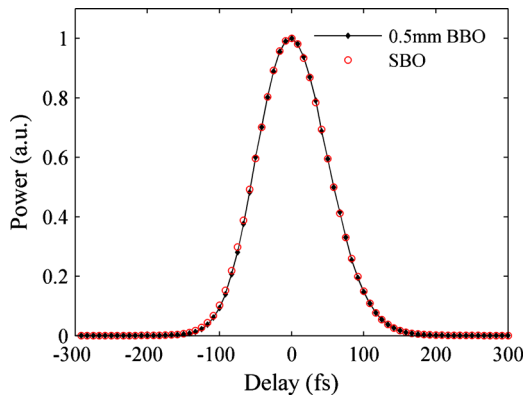


FIG. 4. (Color online) Autocorrelation functions obtained using NPC SBO ($\tau=82.1$ fs, $P_{\text{NLDVB}}=4.72$ μW) and 0.5 mm thick BBO ($\tau=81.8$ fs, $P_{\text{BBO}}=850$ μW).

In case of angular phase matched reference crystal, the average power of autocorrelation signal P_{BBO} was approximately 200 times higher than in case of NLDVB in SBO, which is understandably due to the high randomness of the latter.¹⁴ One may expect that this loss in power will be accompanied by the increase in tuning range of measured laser sources and by the angular detuning tolerance. Large randomization is not only the factor that enables observation of NLDVB in a wide-angle range but it also allows adjustment of better signal-to-noise ratio. The measured contrast between maximum signal and background in Fig. 4 is 1600 for NPC SBO and 21 100 for BBO. At the same time, the background in the measurement using BBO (40 nW) appeared to be more than ten times higher than that in case of NPC (3 nW). The contrast in our measurement is also much better than in another autocorrelation experiment with random media.³

We additionally performed autocorrelation measurements at two different central wavelengths of oscillator, namely, 760 and 780 nm. These measurements were performed at the same conditions as for 800 nm, without any tuning of NPC. The results are quite similar to those for 800 nm central wavelength.

In conclusion, we observed nonlinear diffraction from virtual beam in random NPC of strontium tetraborate for two

different geometries. NLDVB is continuously observable in a wide range of NPC rotation angles. The accuracy of autocorrelation measurements using this effect is as high as in case of angular phase matching. The tuning of central wavelength does not require the adjustment of nonlinear medium. NPCs of SBO are promising materials for pulse diagnostics in a short-wavelength range.

The work was supported by Ministry of Education and Science of Russian Federation (Contract No. 16.740.11.0150); Grant of President of Russian Federation for support of leading scientific schools Grant No. SS-4645.2010.2; Grant No. RNP.2.1.1.3455 and Projects 2.5.2 and 3.9.1 of PSB RAS; and Projects Nos. 27.1 and 5 of SB RAS. A.M. Vyunishev is grateful for support from Carl Zeiss Grant and from Krasnoyarsk Regional Fund of Science and Technical Activity Support.

¹J.-C. Diels and W. Rudolph, *Ultrafast Laser Pulse Phenomena* (Elsevier/Academic Press, New York, 2006).

²R. Trebino, A. Baltuska, M. S. Pshenichnikov, and D. A. Wiersma, in *Few-Cycle Laser Pulse Generation and Its Applications*, edited by F. X. Keartner (Springer, Berlin, 2004).

³R. Fischer, D. N. Neshev, S. M. Saltiel, A. A. Sukhorukov, W. Krolikowski, and Yu. S. Kivshar, *Appl. Phys. Lett.* **91**, 031104 (2007).

⁴D. Dumay, S. M. Saltiel, D. N. Neshev, W. Krolikowski, and Y. S. Kivshar, *J. Phys. B* **42**, 175403 (2009).

⁵A. I. Zaitsev, A. S. Aleksandrovskii, A. V. Zamkov, and A. M. Sysoev, *Inorg. Mater.* **42**, 1360 (2006).

⁶V. Petrov, F. Noack, D. Shen, F. Pan, G. Shen, X. Wang, R. Komatsu, and V. Alex, *Opt. Lett.* **29**, 373 (2004).

⁷A. I. Zaitsev, A. S. Aleksandrovsky, A. D. Vasiliev, and A. V. Zamkov, *J. Cryst. Growth* **310**, 1 (2008).

⁸A. S. Aleksandrovsky, A. M. Vyunishev, A. I. Zaitsev, A. V. Zamkov, and V. G. Arkhipkin, *J. Opt. A, Pure Appl. Opt.* **9**, S334 (2007).

⁹A. S. Aleksandrovsky, A. M. Vyunishev, V. V. Slabko, A. I. Zaitsev, and A. V. Zamkov, *Opt. Commun.* **282**, 2263 (2009).

¹⁰A. S. Aleksandrovsky, A. M. Vyunishev, I. E. Shakhura, A. I. Zaitsev, and A. V. Zamkov, *Phys. Rev. A* **78**, 031802(R) (2008).

¹¹A. S. Aleksandrovsky, A. M. Vyunishev, A. I. Zaitsev, and V. V. Slabko, *Phys. Rev. A* **82**, 055806 (2010).

¹²S. M. Saltiel, D. N. Neshev, W. Krolikowski, N. Voloch-Bloch, A. Arie, O. Bang, and Y. S. Kivshar, *Phys. Rev. Lett.* **104**, 083902 (2010).

¹³W. Wang, Y. Sheng, Y. Kong, A. Arie, and W. Krolikowski, *Opt. Lett.* **35**, 3790 (2010).

¹⁴R. Fischer, S. M. Saltiel, D. N. Neshev, W. Krolikowski, and Yu. S. Kivshar, *Appl. Phys. Lett.* **89**, 191105 (2006).